J. Membrane Biol. 210, 199–212 (2006)
DOI: 10.1007/s00232-006-0858-8

The Journal of
Membrane
Biology

Strengths and Limits of Beta Distributions as a Means of Reconstructing the True Single-Channel Current in Patch Clamp Time Series with Fast Gating

I. Schroeder, U.-P. Hansen
Center of Biochemistry and Molecular Biology (ZBM), Leibnizstr. 11, 24098, Kiel, Germany

Received: 16 November 2005/Revised: 20 March 2006

Abstract. Single-channel current seems to be one of the most obvious characteristics of ion transport. But in some cases, its determination is more complex than anticipated at first glance. Problems arise from fast gating in time series of patch-clamp current, which can lead to a reduced apparent (measured) single-channel current. Reduction is caused by undetected averaging over closed and open intervals in the anti-aliasing filter. Here it is shown that fitting the measured amplitude histograms by Beta distributions is an efficient tool of reconstructing the true current level from measured data. This approach becomes even more powerful when it is applied to amplitude distributions-per-level. Simulated time series are employed to show that the error sum is a good guideline for finding the correct current level. Furthermore, they show that a Markov model smaller than the one used for gating analysis can be used for current determination (mostly O-C, i.e., open-closed). This increases the reliability of the Beta fit. The knowledge of the true current level is not only important for the understanding of the biophysical properties of the channel. It is also a prerequisite for the correct determination of the rate constants of gating. The approach is applied to measured data. The examples reveal the limits of the analysis imposed by the signal-to-noise ratio and the shape of the amplitude distribution. One application shows that the negative slope of the *I-V* curve of the human MaxiK channel expressed in HEK293 cells is caused by fast gating.

Key words: Anti-aliasing filter — Beta distributions — Distributions-per-level — Fast gating — Flickering — Hidden Markov models — MaxiK — Negative slope — Single-channel current — Temporal resolution

Introduction

The transport properties of ion channels are of crucial importance for living cells. Their physiological function is determined by channel number, single-channel current and gating behavior, i.e., by spontaneous or agent-induced transitions between conducting and non-conducting states. Short-term effects of the adaptation to metabolic requirements are mostly achieved by modulation of gating (Tamargo et al., 2004). Also, many chanellopathies are due to a change in gating (Shieh et al., 2000; Lehmann-Horn & Jurkat-Rott, 1999).

Prior to the investigation of the effects on single-channel current, a distinction between permeation and gating effects has to be achieved. A modification of apparent current by a permeation effect would imply that the (average) time between the transitions of two ions is changed. In the case of a gating effect, the statistical characteristics of ion transition remain unchanged for a certain time interval, called open event, but the individual open events are separated by sojourns of the channel in a closed (non-conducting) state (Hansen, Keunecke & Blunck, 1997; Townsend & Horn, 1999).

In many experiments, the distinction between a gating effect and a permeation effect is not trivial. There are several reports that gating may be very fast with mean dwell times in the open or closed state of 1–10 μs (Heinemann & Sigworth, 1991; Parzefall et al., 1998; White & Ridout, 1998; Zheng, Venkataramanan & Sigworth, 2001; Schroeder et al., 2004, 2005) or even less (Weise & Gradmann, 2000).

Abbreviations: a. u., arbitrary units; HMM-fit, direct fit of the time series; SQ-fit, subsequent HMM- and Beta-fit; O, open state; O_t, true single channel current; O_a, apparent single-channel current; C, closed state; SNR, signal-to-noise ratio.

Correspondence to: U.-P.Hansen; email: uphansen@zbm.uni-kiel.de

Averaging over very short closed and open intervals occurs in the inevitable anti-aliasing filter, thus leading to an apparent reduction of single-channel current.

The correct knowledge of the true current level is not only important for revealing the mechanism of the action of drugs and messengers. It is also an important parameter in the investigation of the biophysical behavior of the channel. Firstly, it is a measure of the efficiency of a channel to translocate ions. This value may be a keystone for predictions of Molecular Dynamics calculations. Secondly, the correct value of single-channel current is required for the analysis of gating. Below, an example is given which shows that the assumption of a false current level also leads to false rate constants of the assumed Markov model. Apparent (i.e., measured) current levels that deviate from the true single-channel current can originate from fast gating (Hille, 1992; Hansen et al., 1997; Townsend & Horn, 1999).

There are several approaches to determine single-channel current from measured patch-clamp data. Riessner et al. (2002) investigated the efficiency of three different approaches: 1. Fitting the amplitude histogram with gaussians. 2. Evaluation of the time series on the computer screen (fit-by-eye). 3. An automatic procedure searching for jump-free sections in the time series and sorting them according to length and frequency of occurrence. Using simulated data, Riessner et al. (2002) found that the fit-by-eye and the automatic detector gave better results than the fit of the amplitude histogram by gaussians.

However, the three approaches tested by Riessner et al. (2002) can only be employed if the sojourns in the open and closed states are long enough, i.e., longer than the averaging time of the inevitable anti-aliasing filter. If fast gating and averaging of open and closed times in the anti-aliasing filter diminishes the measured single-channel current, the true value would remain hidden.

Venkataramanan and Sigworth (2002) included the value of single-channel current in their fitting routines using a highly elaborated version of the direct fit of the time series (HMM fit). Huth (2005) suggested to use 2-D dwell-time histogram fits. He showed that the shape of the reconstructed amplitude histogram was sensitive to the correct choice of the true single-channel current.

Here, a simpler approach requiring less computing time is proposed which can find the true current value even if fast gating has led to a reduced apparent current level. This is achieved by fitting the amplitude histograms by Beta-distributions (FitzHugh, 1983; Yellen, 1984; Klieber & Gradmann, 1993; Riessner, 1998). The approach utilizes the effect that averaging over fast gating causes deviations of the amplitude histogram from one that is merely shaped gaussian caused by noise. These deviations carry information about the rate-constants of the involved Markov process.

The first analytical methods to calculate theoretical beta distributions were restricted to two-state models with first-order filters (FitzHugh, 1983, Klieber & Gradmann, 1993). Yellen (1984) proposed a correction factor for higher-order filters. Heinemann and Sigworth (1991) examined the higher-order cumulants of open-channel noise, but this method required some rather strict assumptions about the gating (very short and infrequent gaps). Riessner (1998) developed an analytical algorithm to evaluate Hidden Markov models with more than two states and more than one channel. However, this analysis was also restricted to first-order filters which have little relevance in patch-clamp analysis. Correction factors did not solve the problem in the case of multi-state models (probably also not in the case of two-state models, Riessner, 1998).

White and Ridout (1998) designed a method for fitting amplitude histograms which already comprised multi-state Markov models and higher-order filters. They calculated the theoretical beta distribution by considering all possible state sequences within the filter rise time (*see* also Appendix).

Here, an alternative method is proposed. The increased computer power since 1998 rendered possible the use of simulations to generate artificial time series for the construction of the theoretical amplitude histograms originating from higher-order filters and multi-state multi-channel models. This approach is very powerful because all features of noise and filtering can easily be implemented. In contrast to the above mentioned papers, the investigations here do not aim for rate constants. Instead, the beta fit is used to reconstruct the (a priori unknown) single-channel current.

Materials and Methods

Electrophysiological Measurements

Patch-clamp measurements were performed under steady-state conditions on inside-out patches of HEK293 cells, stably expressing an h-MaxiK α-GFP construct and the β1 subunit (Moss and Magleby, 2001; Shi & Cui, 2001). The cells were a gift from Prof. U. Seydel and Dr. A. Schromm, Research Center Borstel. The pipette solution contained 150 mM KNO_3, 2.5 mM $Mg(NO_3)_2$, 2.5 mM $Ca(NO_3)_2$, 10 mM HEPES/KOH, pH = 7.2. The solutions in pipette and bath were identical, if not otherwise stated.

The experimental set-up is described in detail by Draber and Hansen (1994). Briefly, electrodes were made from borosilicate glass (Hilgenberg, Malsfeld, Germany) coated internally with Sigmacote (Sigma, Deisenhofen, Germany), drawn on an L/M-3P-A puller (Heka, Lambrecht, Germany), and filled with the solution mentioned above. The pipettes were dried at 55°C overnight after pulling. This treatment increased seal probability and resistance (Huth, 2005). Patch-clamp current was recorded by a Dagan 3900A amplifier (Dagan, Minneapolis, MN) with a 4-pole anti-aliasing

filter of 50 kHz. Data were stored on disk with a sampling rate of 200 kHz.

Distributions-per-level

Distributions-per-level were generated as described previously in Schroeder et al. (2005): A Hinkley-Detector (Schultze & Draber, 1993) was used to reconstruct the jump-free time series. All data points were grouped according to their assignment by the detector to the different current levels. From each level, a separate amplitude histogram was built, including filter response and missed events. Thus, missed events corrections (Milne et al., 1989; Crouzy & Sigworth, 1990; Draber & Schultze, 1994) are not required.

Multi-state Multi-channel Beta Distributions for Higher-order Filters

The theoretical amplitude distributions needed for the fitting algorithms were generated as follows: First, a single-channel time series was simulated as described in the Appendix, and the amplitude histogram was constructed by standard procedures. Multi-channel amplitude distributions (A_N) were calculated iteratively by means of convolution

$$A_N(I) = \int_{-I_{max}}^{I_{max}} A_1(u) \cdot A_{N-1}(I-u)du \tag{1}$$

with A_1 being the amplitude distribution for a single channel, $A_{(N-1)}$ the distribution for N-1 channels, and u the integration variable covering the whole range of currents from $-I_{max}$ to I_{max}. Also the amplitude distribution of noise $W(u)$ can be introduced by convolution

$$A(I) = \int_{-I_{max}}^{I_{max}} A_N(u) \cdot W(I-u)du \tag{2}$$

W(u) should not include the noise caused by fast gating. Since the noise of the base line is gaussian, a theoretical distribution can be used with the variance of $W(u)$ obtained from a jump-free section of the time series. Such a section could always be obtained in all our investigations on human MaxiK channels or the dominant K^+channel in *Chara*, because the related 5-state Markov model had long-living closed states (Farokhi, Keunecke & Hansen, 2000; Hansen et al., 2003; Schroeder, Diddens & Hansen, *in preparation*).

In all simulations, the corner frequency of the anti-aliasing 4-pole Bessel filter is set to 50 kHz, and the sampling rate is 200 kHz as commonly used in our group for the investigation of fast gating (Farokhi et al., 2000; Hansen et al., 2003).

Curve Fitting

Fitting theoretical Beta distributions to measured amplitude histograms on the basis of an assumed Markov model minimizes

$$\text{error sum} = \sum_{i=1}^{N_I} \frac{(A_{\text{exp},i} - A_{theo,i})^2}{A_{\text{exp},i} + 0.1} \tag{3}$$

$A_{\text{exp,i}}$ is a data point in the amplitude histogram obtained from the measured time series. $A_{\text{theo,i}}$ is a "theoretical" data point in the amplitude histogram obtained from the time series simulated from an assumed Markov model as described in the Appendix. N_I is the number of data-points in the amplitude histograms (number of intervals on the current-axis, in our case 4096). The denominator prevents that the maximum values of the amplitude histogram get the highest weight. The highest values are close to gaussian distribution, whereas the deviations carrying the information about fast gating are found at the slope of the distribution. 0.1 is added in order to prevent overflow resulting from division by zero.

The procedure is time consuming as each step of the simplex algorithm (Caceci & Cacheris, 1984; Press et al., 1987) requires one simulation of the time series. However, there is the advantage of Eqs. 1 and 2, which implies that multi-channel Beta distributions can be obtained from convolution of single-channel distributions. Thus, they do not require the time-consuming simulation of a macro-channel including the m^N states of an m-state N-channel scenario as in the direct fit of the time series (HMM fit, Albertsen & Hansen,1994).

Other Fitting Routines Used

HMM-fit: direct fit of the time series (Fredkin & Rice 1992). The version used here (Albertsen & Hansen, 1994) does not account for filter effects. This results in the underestimation of fast rate constants.

SQ-Fit: Subsequent fit of the time series (HMM-fit) and of the amplitude histogram with beta distributions (Schroeder et al. 2005). The slow rate constants are inherited from the HMM-fit. The fast ones are determined by the subsequent beta fit.

Results

Illustrating the Necessity of Knowing the True Current

The time series shown in Fig. 1*A* is used to demonstrate the necessity of knowing the true current level when the rate constants of the underlying Markov model are to be determined. In most patch-clamp records with fast gating, only the apparent current level is observed. Fortunately, in our experiments on MaxiK, there were some rare records where sojourns in the open state were so long, that the true level was reached. The time series in Fig. 1*A* belongs to this kind of record. It is an especially suitable example because these sojourns in the true level were so seldom that they may have been overlooked, thus mimicking the situation found in most experiments.

Here, we consider two scenarios: 1) The experimenter is aware of the short sojourns in the true open level and 2) only the apparent current level is observed. For the kinetic analysis in both scenarios, the linear 5-state Markov model

$$O1 \rightleftharpoons O2 \rightleftharpoons C3 \rightleftharpoons C4 \rightleftharpoons C5 \tag{4}$$

was used, which worked fine with all our human MaxiK data and its analog in *Chara* (Farokhi et al. 2000; Hansen et al. 2003).

The measured time series was fitted by means of the *SQ*-fit with the current level taken from the rare sojourns in the slow open state (O_t in Fig. 1*A*) or from the apparent current level (O_a). The rate constants obtained from this analysis were used to construct the related simulated time series. The comparison of Figs. 1*A* and *B* shows that the

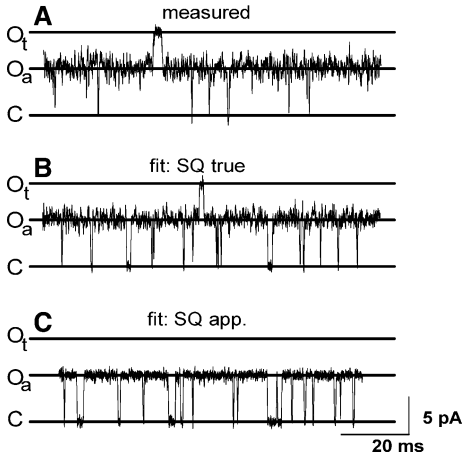

Fig. 1. (*A*) Measured time series from h-MaxiK at +200 mV sampled at 200 kHz presented with a 20-point moving average filter. Gating is very fast, resulting in the apparent open level O_a. Sometimes, the true open level O_t becomes visible. (*B*, *C*) Time series simulated from the rate constants of the best *SQ*-Fit (*B*) with the true current level O_t, (first row in Table 1; average of the best 10 out of 20 fits), (*C*) with the apparent current level O_a (17 out of 25; rate constants not shown but similar to those in row 3 of Table 1).

measured time series and that one simulated under scenario 1 look very similar, as expected. Especially, the rare sojourns in the true current level are well reproduced. This verifies that both levels in Fig. 1*A* originate from the same original current level. In contrast, scenario 2, using the apparent (wrong) current level, inevitably yields rate constants that produce a quite different time series (Fig. 1*C*).

Even though visual inspection of time series may give a first hint that an analysis has failed (Fig. 1*C*), a more quantitative illustration of the effect of an incorrect current estimation is presented in Table 1 and Fig. 2. Simulated data are used to show that fits under scenario 2 yield incorrect rate constants of the Markov model. The simulated time series was generated from the rate constants obtained from the *SQ*-fit of the measured time series (first row in Table 1). It is, of course, identical to the time series in Fig. 1*B*. This time series (which now replaces the measured one in Fig. 1*A*) was fitted by

- the *SQ* fit assuming the true correct level (scenario 1)
- the *SQ* fit with the apparent current level (scenario 2).

The results are shown in Table 1, second and last row.

The *SQ*-fit assuming the correct current level should reproduce the rate constants used for simulation. However, there are some deviations due to the superimposed noise and insufficient lengths of time series. The rate constants of the O-C transition are a bit overestimated, but it has to be kept in mind that they are more than ten-fold faster than the anti-aliasing filter (50 kHz). The rate constants between the two open states are wrong by a factor of two. This is due to the extreme low occupation probability of $O1$ (below 0.3 %), providing not enough events to reach the statistic equilibrium. In contrast, the results obtained by fitting with the apparent current level (scenario 2) are completely wrong, in some cases by several orders of magnitude.

In the case of measured time series, the experimenter does not know the true rate constants, thus the detection of wrong rate constants cannot serve as an indicator of wrong current levels. Figure 1*C* shows that the comparison of the measured time series and that one simulated from the fit results may give a first hint that something is wrong. However, a more powerful analysis should be based on beta distributions, which serve a double purpose: helping to find the true current level and detecting a failure of the analysis. The utilization of beta distributions to determine the true current before the analysis by the SQ-fit or other methods of determining the rate constants is described in the next sections.

The second feature is illustrated in Fig. 2, which shows the full amplitude histograms of the time series simulated from the rate constants in Table 1. Because of the bad SNR, only one peak is visible. The SNR was 4 when calculated for the apparent current level and 12.4 for the true level. Figure 2 shows that the amplitude histogram constructed from the rate constants obtained from fitting with the true level (row 2 in Table 1) coincides very well with that one of the measured original time series (row 1 in Table 1), whereas a clear deviation becomes obvious in the case of the amplitude histogram obtained from the fit results using the apparent current level (row 3 in Table 1).

Relationship between Beta Distributions and Current Reduction

The reduction of single-channel current by fast gating is illustrated in Fig. 3. Simulated time series were used to demonstrate that the same apparent single-channel current can be produced by quite different true single-channel currents. The degree of current reduction depends on the parameters of the gating process. For the illustration of this effect, time series were generated using the following Markov model:

$$O \underset{x\cdot 5\cdot 10^5 s^{-1}}{\overset{5\cdot 10^5 s^{-1}}{\rightleftharpoons}} C \qquad (5)$$

All these simulations resulted in the same apparent open-channel current, even though quite different true current levels were used for simulating the time series. The choice of the kinetic parameters in Eq. 5 was the origin of the current reduction. This is indicated by the very different curve shapes of the amplitude distributions. In other words, measuring an apparent single-channel current does not always

Table 1. Rate constants in s^{-1} obtained from the simulated time series of Fig. 1*B* with the two different fitting strategies (best error sum out of ten fits, respectively) described in the text

Fit strategy	k_{O1O2}	k_{O2O1}	k_{O2C3}	k_{C3O2}	k_{C3C4}	k_{C4C3}	k_{C4C5}	k_{C5C4}
Simulated	4237	24	575472	787231	1053	4987	73	396
SQ true (scenario 1)	2169	12	760439	1103290	1243	4349	55	325
SQ app. (scenario 2)	1834	1151	2982	126734	44200	5448	78	368

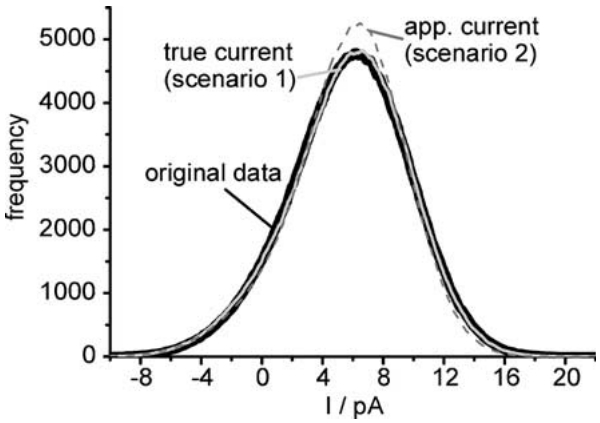

Fig. 2. Amplitude histograms generated from time series simulated from the three sets of rate constants presented in Table 1. *Very thick black curve*: Rate constants used for the "original" time series (first row in Table 1. The thickness of the curve is not caused by noise, but chosen for better demonstration of the coincidence of the curves). *Continuous grey curve*: Rate constants obtained from the *SQ*-fit of the "original" (simulated) data with the correct single-channel current. *Dashed grey curve:* Rate constants obtained from the *SQ*-fit using the apparent single-channel current. In both scenarios, the fit with the best error sum (Eq. 3) out of ten runs is shown.

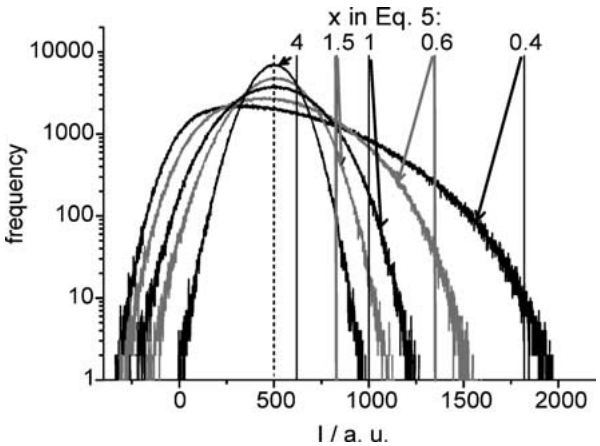

Fig. 3. Different curve shapes lead to different true single-channel currents. Time series were simulated which resulted in the same apparent single-channel current (dashed *vertical line*), but which had different rate constants of fast gating (*see* labels and Eq. 5) and different true currents (solid vertical lines). Sampling frequency: 200 kHz, filter frequency: 50 kHz.

yield the true single-channel current. Below, details of the technique of reconstructing the true current level from the amplitude histogram of a measured time series are presented. Simulated and measured data are used to test the performance of the algorithms.

Successful Reconstruction of the Current Level Requires Distributions-per-Level

As implicated by Fig. 3, the true current level can be obtained by fitting the amplitude histogram with beta distributions. The following example shows that the efficiency of the approach can be strongly increased by using distributions-per-level (*see* Materials and Methods and Schroeder et al., 2004) instead of the overall amplitude histograms.

Distributions-per-level have been used by different authors for different purposes. They occur in the prediction equation of the direct fit of the time series (HMM fit, Fredkin & Rice 1992; Albertsen & Hansen, 1994). Other examples are visualization and comparison of baseline and open-channel noise, e.g., Weise & Gradmann (2000) and Rosenmund, Stern-Bach & Stevens (1998). Their usefulness for model identification has been discussed by Schroeder et al. (2004).

Figure 4*A* shows a simulated record, including fast gating. The two levels that can be seen are the closed level and the apparent open level. The true open level (indicated by the horizontal line "O") is hidden. The apparent open state includes sojourns in the fast open and in the fast closed state. Thus, the apparent level and the excess noise result from averaging over these states. The visible sojourns in the closed state are caused by long events related to a second slower closed state. By means of distributions-per-level, the fast O-C transition can be separated from the sojourns in the slow closed state. This enables the usage of a simpler model for the fit of the beta distributions.

The benefit of this approach is illustrated by means of the time series in Fig. 4*A*. It was generated from the following model (rate constants in s^{-1}):

$$O \underset{2\cdot10^5}{\overset{1\cdot10^5}{\rightleftharpoons}} C \underset{200}{\overset{1000}{\rightleftharpoons}} C \qquad (6)$$

The true current value in the simulation was 500 a.u., the resulting apparent current was 400 a.u.

The final goal is the reconstruction of the true current. The fitting routine employs two sets of variables, one set for the rate constants and one for the current. In order to show the strong dependence of the error sum on the assumed current value, we use a parametric approach for Fig. 4 instead of fitting all parameters simultaneously. In the following series of fits, the current is kept constant at different values, and we use the fit only for the determination of the rate constants.

Four different fitting strategies were tested. For each strategy, fits were done at different current levels.

1. The fit tries to approximate the over-all amplitude histogram on the basis of the correct *OCC*-Model (*filled squares* in Fig. 4*B*, *C* and *D*). This works fine; both rate constants and the current are determined correctly. However, the problem arises that the Beta fit often becomes unstable with more than two states (as implicated by the error bars e. g. in Fig. 4*D*).

2. The fit tries to approximate the over-all amplitude histogram on the basis of a reduced *OC*-Model. The error sum becomes minimum at a wrong current value and the rate constants are misestimated (*empty circles* in Fig. 4*B*, *C* and *D*).

3. The fit assumes the reduced *OC*-Model. In contrast to the above two approaches, not the whole amplitude histogram, but only the apparent *O*-distribution is fitted. The Hinkley-detector was set to the apparent current level (400 units, *upright triangles*)

4. Same as strategy 3, but the Hinkley detector was set to the true level (500 units, *inverted triangles*). Strategies 3 and 4 both estimate the current and the rate constants with good accuracy.

The fit of the over-all amplitude histogram is sensitive to the choice of the correct model, as becomes obvious from curve 2 (*empty circles* in Fig. 4*B*, *C*, *D*). This problem can be overcome by using distributions-per-level. The results show that fitting distributions-per-levels is tolerant to the usage of reduced models. This is of great advantage because complex models lead to instabilities when fitting beta distributions. From the comparison of the results of strategies 3 and 4, we can also conclude that this approach is quite robust with respect to the settings of the Hinkley detector, which is important for the application to measured data, when fast flickering impairs the assignment of current levels.

Testing the Level Fit

Above, it was shown that the error sum of the beta fit yields a sharp minimum when the correct true current level is assumed. The full version of the fitting program (''beta_leveldetektor'' at www.zbm.uni-kiel.de/software) optimizes both parameter sets: rate constants and current level, in contrast to the investigations in Fig. 4. The performance of this fit algorithm (as described in Materials and Methods) is tested on three simulated time series which showed apparent current reduction. The test comprises the following steps:

1. Simulation of the time series

2. Generation of the apparent open-distribution from the time series (distribution-per-level)

3. Fitting Beta-distributions to the open-distribution, with the current and the rate constants as free parameters

The models used for simulation are (rate constants in s^{-1}):

$$O_{(0.25/10\mu s)} \underset{200{,}000}{\overset{100{,}000}{\rightleftharpoons}} C_{(0.125/5\mu s)} \underset{200}{\overset{1000}{\rightleftharpoons}} C_{(0.625/5000\mu s)} \tag{7}$$

$$O_{(0.12/20\mu s)} \underset{10{,}000}{\overset{50{,}000}{\rightleftharpoons}} O_{(0.59/9\mu s)} \underset{300{,}000}{\overset{100{,}000}{\rightleftharpoons}} C_{(0.20/3.3\mu s)} \underset{1000}{\overset{500}{\rightleftharpoons}} C_{(0.10/1000\mu s)} \tag{8}$$

$$O_{(0.12/1\mu s)} \underset{500{,}000}{\overset{1{,}000{,}000}{\rightleftharpoons}} C_{(0.24/1.8\mu s)} \underset{10{,}000}{\overset{5{,}000}{\rightleftharpoons}} C_{(0.12/93\mu s)} \underset{200}{\overset{700}{\rightleftharpoons}} C_{(0.41/5000\mu s)}$$
$$100{,}000 \uparrow\downarrow 50{,}000$$
$$O_{(0.12/10\mu s)} \tag{9}$$

The steady-state occupation probabilities of the states and their individual lifetimes are given in brackets above the state symbols in Eqs. 7 to 9. The first model (Eq. 7) corresponds to that one used in Fig. 4*A* (Eq. 6). Here, it is tested whether the minimum in Fig. 4*C* can automatically be found by the full version of the program.

All simulations used a true current of 500 a.u. The resulting apparent currents are given in Table 2. Also given in the table are the true and the fitted values of the current, the *C*-*O* and *O*-*C* rate constants.

The omission of the slow *C*-state in the model of Eq. 7 (first row in Table 2) does not impair the accuracy of the fit. The current level and the rate constants come close to the values used for the simulations.

Good results are also obtained for the case of the linear model of Eq. 8. Replacing the two open states by one results in the correct current level, and also the rate constants are acceptable. Using both open states (*OOC*, row 3 in Table 2) only minimally improves the quality of the fit, showing that fitting by a reduced model is legitimate.

The situation is different for the branched model (Eq. 9, *OOCCC*, rows 4 and 5 in Table 2). It serves as an example where the estimation of the true current is reasonably correct but the rate constants have to be refitted by another fitting program.

Fitting an *OC*-model to the open-distribution results in a true single-channel current that is about

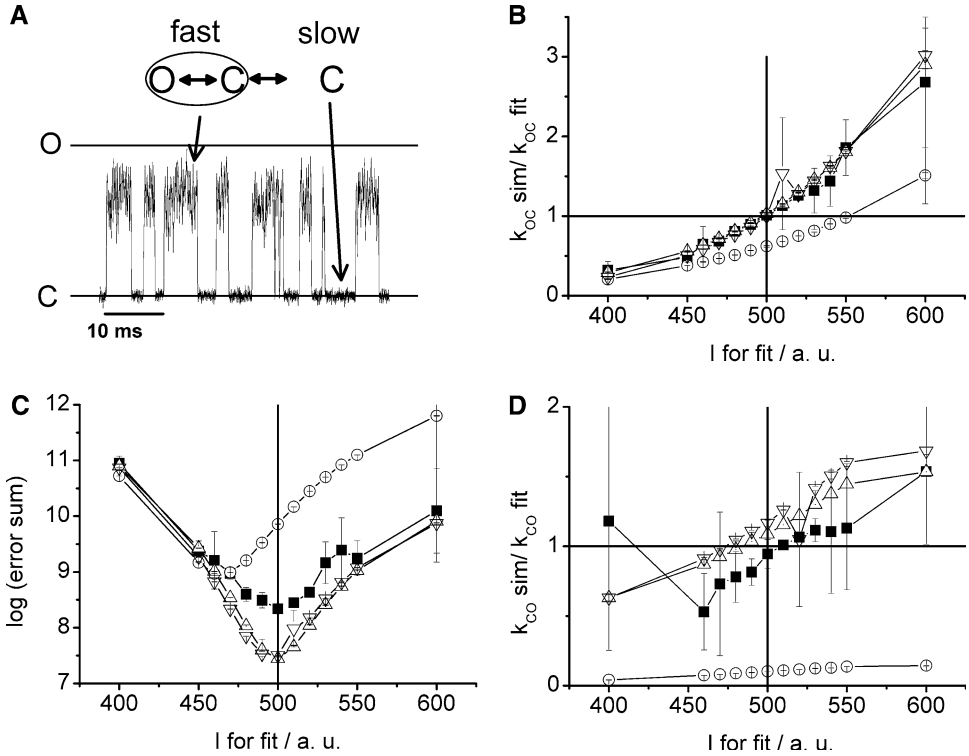

Fig. 4. Finding the correct current level. A time series was simulated with true current level (500 a.u.) from the *OCC*-model in Eq. 6 and the influence of the assumed current on the error sum of the beta fits are investigated. Each data point presents the average of three runs. Four different fit strategies were employed to adjust the rate constants, but not the fixed current given at the abscissa: The over-all amplitude histogram was fitted with the correct OCC-model (■) or a reduced *OC*-model (○). Both triangles were obtained from fitting the noisy apparent *O*-level (distributions-per-level in (*A*)) with the reduced *OC*-model. The two curves differ by the current setting of the Hinkley detector. One uses the apparent current level (400 units, Δ) and the other one, the true level (500 units, ▽). The parameters used for the simulation are represented by horizontal (rate constants) and vertical (current) lines. (*A*) The apparent flickery open level is formed by the fast *O*-*C*-transition. (*C*) Error sums. (*B*) and (*D*) Rate constants.

10% higher than the nominal value (row 4 in Table 2). Including the second open state into the fit again does not improve the accuracy (last row in Table 2). The bias of 10% may be tolerable. The rate constants k_{OC} and k_{CO} obtained from fitting with the reduced model (column 3 in Table 2) are different from those used for the simulations of the time series. Using the more correct *OCO*-model yields a slightly better current estimation. Also the slower *O*-*C*-transition can be identified (simulated: 100 and 50 kHz, fitted: 149 and 66 kHz, respectively), but the rate constants of the fast *O*-*C*-transition have little relation to the simulated model (simulated: 1000 and 500 kHz and fitted: 301 and 355 kHz, respectively).

The resulting message is that the true current level is correctly reconstructed by the fit, even though the estimation of the rate constants may be poor. In a real experiment, the experimenter cannot check the influence of the usage of the reduced model on the fitted rate constants. Thus, it is recommended to use the true single-channel current obtained from the analysis described above for a new *SQ*-fit (Schroeder et al., 2005) in order to determine the rate constants.

Time Series with Two Channels

In order to demonstrate the performance of true-level reconstruction for more than one channel, a time series was simulated from the *OCC*-model of Eq. 7 with two identical channels. Fast gating causes current reduction in both open levels. For the reconstruction of the true current level, distributions-per-level were constructed as shown in Fig. 5*A*. The distributions of the *C* and the *O* level show bulges at the right-hand slope which result from missed transitions to the higher current level (Schroeder et al. 2004). The distribution-per-level for two channels open (*2O* in Fig. 5*A*) shows a clear asymmetric beta distribution which seems to be most suitable for the reconstruction of the true current.

Fitting of distributions-per-level with Beta distributions has an inherent problem: It has a tendency to end up in local minima. Variability of the fitting results, which is useful to overcome this problem, can be introduced by the choice of the starting values for the rate constants k_{CO} and k_{CO} and the current *i*. Further variability is introduced by the randomness

Table 2. Influence of the usage of a reduced model (second column) for fitting distributions-per-level from different simulated time series. The parameters obtained from the fits with the smallest error sums are given with SEM (on average, 18 out of 30 fits were successful for each model)

Simulated model	Fitted model	Apparent current	True current	Fitted current	k_{OC} sim/ms^{-1}	k_{CO} sim/ms^{-1}	k_{OC} fit/ms^{-1}	k_{CO} fit/ms^{-1}
OCC (Eq. 7)	OC	400	500	501 ± 2	100	200	103 ± 3	230 ± 4
OOCC (Eq. 8)	OC	440	500	504 ± 1	100	300	86 ± 1	310 ± 2
OOCC (Eq. 8)	OOC	440	500	500 ± 1	100	300	102 ± 5	322 ± 4
OOCCC (Eq. 9)	OC	350	500	553 ± 5	1000; 100	500; 50	271 ± 11	408 ± 8
OOCCC (Eq. 9)	OCO	350	500	536 ± 15	1000; 100	500; 50	301 ± 27; 149 ± 53	355 ± 49; 66 ± 49

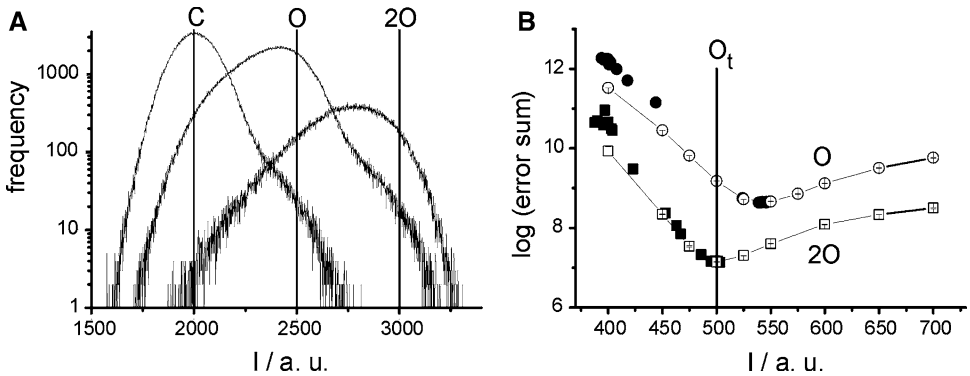

Fig. 5. Test of the level fit for time series simulated with two channels of the *OCC*-model of Eq. 7. The time series showed current reduction by fast gating in both open levels. (*A*) Distributions-per-level related to the three apparent levels. The true current levels of the closed state (*C*), of one (*O*) and two open channels (*2O*) are given by vertical lines. (B) Dependence of the error sum on the estimated current. Upper curve (*circles*): The *O*-distribution was fitted with one *OC*-channel. Lower curve (*squares*): The *2O*-distribution was fitted with two *OC*-channels. Closed symbols: fits with the current as a free parameter. Open symbols: fit with the current as fixed parameter. The true current O_t is indicated by the verticl line.

of the generation of the time series which serves to create the ''theoretical'' Beta distribution (Eqs. 1 and 2).

Fortunately, as shown in Fig. 4*C*, the error sum is a helpful guide to find the global minimum. Plotting the error sum of the fits versus the estimated current shows that the error sum obtains a clear minimum at the true single-channel current (which is known in simulated data and is indicated by a vertical line in Fig. 5*B*). The suitability of the error sum as a guide line in the totally free fit (rate constants and current are free parameters, presented by *filled symbols* in Fig. 5*B*,) was tested by the comparison with fits with fixed current (*empty symbols* in Fig. 5*B*). The results of both approaches coincided.

The fit of the *2O*-level gave a clear minimum at the true current level (*squares* in Fig. 5*B*, 8 out of 30 fits reached the optimum), whereas the fit of the *O*-level results in a minimum at a current value which was 10 % too high (*circles* in Fig. 5*B*; 12 out of 30 runs reached the minimum). The reason for the different performance of these two fits becomes obvious from Fig. 5*A*. The distribution-per-level for the *2O*-level looks like a smooth Beta distribution, whereas the curve shape of the distribution of the *1O*-level is distorted by events missed by the Hinkley detector. Values which probably should have been assigned to the higher level occur in the distributions of the *C*- and *1O*-levels. This increases the deviation from the gaussian shape, especially at the right-hand slope and pretends a higher true current.

The results of Fig. 5 lead to the following conclusions. 1. Multi-channel fits are possible, but only the highest level seems to be not distorted by undetected transitions to a higher level, and therefore is most suitable for current reconstruction. 2. The results should be verified by repeating the fits with different starting conditions until a clear minimum is obtained in a graph similar to that in Fig. 5*B*.

Testing the Algorithm on Measured Data

Testing the algorithms with real measured data is difficult because, in contrast to simulated data, the true single-channel current is usually unknown. Fortunately, we could observe some time series in which both levels occurred, the true one and the apparent one. One of these time series is shown in Fig. 1*A*. Another type of such time series showed mode switching as also reported by Schroeder et al.

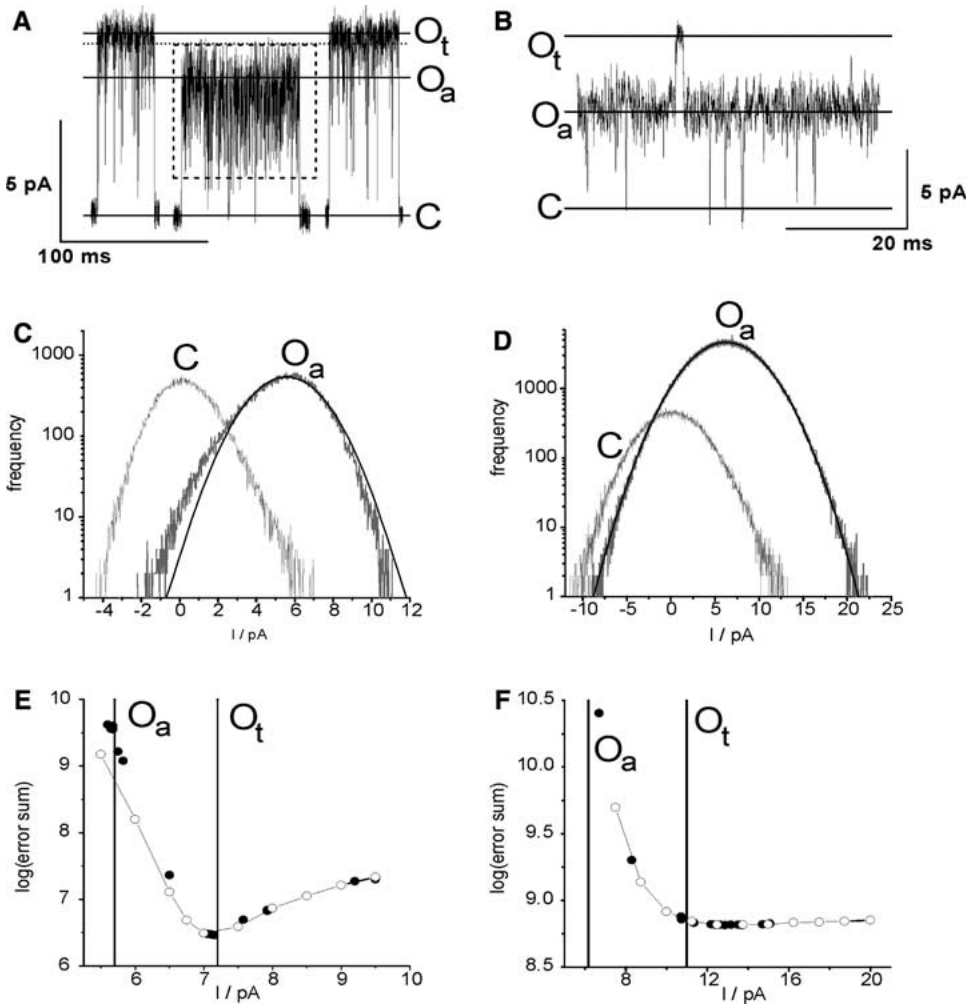

Fig. 6. Time series from h-MaxiK which displayed both the true and the apparent single-channel current that was reduced by fast gating. (*A*) Time series measured at + 60 mV with spontaneous mode switching. There were sections with gating that was so slow that no current reduction occurred (left- and right-hand section) and a section where fast gating reduced the single-channel current (dashed box in the middle). The bath solution contained 100 mM Tl^+ and 50 mM K^+ instead of 150 mM K^+ (*see* Materials and Methods). (*B*) Time series obtained at +200 mV with current reduction by fast gating (O_a = apparent current level) and some rare long sojourns in the true open level (O_t). (*C*) and (*D*) Distributions-per-level for the apparent open (O_a) and the closed state (*C*) from the time series in (*A*) and (*B*), respectively (*grey curves*). The smooth black curves give the best approximation by a gaussian. (*E*) and (*F*) Dependence of the log error sum (Eq. 3) on the estimated current obtaine from different fits of the O_a-distributions in (*C*) and (*D*), respectively. ●: fits with current as a free parameter, ○: fits with fixed current. Vertical lines indicate the true (O_t) and apparent (O_a) current level.

(2004). In the time series displayed in Fig. 6*A*, there were sections in which the ratio of open to closed time within a burst was so high that the true current level appeared at the output of the anti-aliasing filter. However, the channel could spontaneously (and reversibly) switch to another mode where the open probability within the burst decreased (indicated by the 4.5-fold increase of k_{OC} in Table 3), so that current was reduced (section indicated by the dashed box in Fig. 6*A*).

The time series in Fig. 6*A* was used to test whether the true level could be reconstructed from those sections which delivered only the apparent current. As described in the previous section, the distribution of the apparent open-state was generated from the section in the dashed box, showing only the reduced current level (Fig. 6*C*). As discussed above, it is sufficient to use a simple *OC*-model for the fit of the open-histogram (distribution-per-level). Fitting by beta distributions with the current as a free parameter is not straightforward. The fitting routine may end up in local minima. Thus, 20 different fits were done. They differed by the set-file giving the starting value and by the simulated time series because of the randomness of the simulation procedure. Consequently, different estimated current levels were delivered by individual fits. Fortunately, this problem could be overcome by the inspection of the error sum. It helped to find the correct solutions. In Fig. 6*E*, the error sum is

Table 3. Fit results of the two gating modes of the time series in Fig. 6*A*. The mode-switching is caused by a change in a single rate constant (as far as can be seen by the reduced model.) The average is shown for the best 5 fits out of 20 (fast part) and 14 out of 30 (slow part), respectively

	Apparent current	Fitted current	k_{OC}/ms^{-1}	k_{CO}/ms^{-1}
Fast part	5.73 pA	7.14 pA	164 ± 6	510 ± 8
Slow part	7.54 pA	-/-	36 ± 9	504 ± 67

plotted versus the current delivered from the fitting routine. It is obvious that the curve of the error sums takes a minimum very close to the true current of 7.54 pA, which here is fortunately known from the sections of the time series in the "normal" gating mode (Fig. 6*A*, left- and right-hand sections).

In order to test the fitting routine, the beta distribution in Fig. 6*C* (curve O_a) was fitted again under the constraint that the single-channel current was set to a fixed value, and only the rate constants were determined. The resulting error sums coincided with the curve of the completely free fit in Fig. 6*E*, indicating a close relationship between error sum and the quality of estimation of the true single-channel current.

A Caveat Related to Gaussian Distributions

In the time series in Fig. 1*A* (measured at +200 mV), there was no mode switching. Instead it showed the peculiarity that it contained some sufficiently long open events. They allowed the determination of the full single-channel current. The value of 11.1 pA (label "O_t" in Fig. 6*B*) was determined manually by visual positioning of the current level in the raw data, as described in Materials and Methods. The average apparent single-channel current in this record was 6.2 pA (label "O_a" in Fig. 6*B*). Distributions-per-level were constructed for the apparent single-channel current (Fig. 6*D*). This distribution still contained some data points from the long open state. However, their number was so small that they did not influence the curve shape.

The distribution-per-level for the apparent *O*-level is broader than that of the long lasting *C*-levels (Fig. 6*D*). Because of this, it could be expected that this distribution is an effective means of determining the true current level as in the case of the time series in Fig. 6*A*. However, the two curves of the O_a histogram in Fig. 6*D* cannot be distinguished because the measured one coincides perfectly well with a gaussian amplitude histogram. This leads to a caveat which has to be kept in mind when the distribution-per-level becomes gaussian.

Figure 6*F* shows the error sums obtained from 15 free fits and from fits with fixed current level. It does not show a clear minimum. On the left-hand side (at low current values) the error decreases with the estimated current level approaching the true level of 11 pA (which is known from the few sojourns in the true level O_t in Fig. 6*B*). However, for values higher than the true level, the error sum does not increase again as it does in the case of Fig. 6*E*. This bears the following message: In the case of symmetrical gaussian distributions, the fitting routine can only reveal a lower bound for the true current level but cannot exclude values which are too high.

This problem is inherent to the gaussian shape of the distribution in Fig. 6*F*. If gating is much faster than the filter frequency then the distribution always becomes gaussian (Central Limit Theorem, Feller, 1968). In that case, a higher value of the true apparent current can be reduced to the same apparent current by selecting the adequate duty cycle (ratio of open times to closed times). The width of the distribution can be adjusted by the selection of the adequate rate constants. Because of this, the gaussian distribution does not provide enough information to exclude currents which are too high. The situation is more favorable in the case of asymmetrical beta distributions (Fig. 6*C*).

Application: The Negative Slope of MaxiK Is a Gating Effect

There are several phenomena which lead to the question of whether they are brought about by a permeation effect or by fast gating. This holds for sublevels, the anomalous mole fraction effect (AMFE, Farokhi et al., 2000; Hansen et al., 2003; Schroeder, Diddens & Hansen, *in preparation*) and negative slopes of *I-V* curves induced by Cs^+ (Klieber & Gradmann, 1993; Draber & Hansen, 1994) in the MaxiK channel of the tonoplast of *Chara*. Here it is demonstrated that the method of true-current reconstruction by beta distributions can contribute to the solution of this problem.

At higher positive potentials, single h-MaxiK ($\alpha+ß1$) channels in HEK293-cells show a clear negative slope in the *I-V* curve as also found in the case of the MaxiK channels in the plasmalemma of the giant algae *Chara* (Smith, 1984; Beilby, 1985; Tester, 1988). The fit algorithm described above is used to demonstrate that in human MaxiK channels this apparent decrease in conductivity is at least to a major extent a gating effect and not due to a reduction in open-channel conductivity.

The first hint is the phenomenology of the single-channel records shown in Fig. 7*A*,*B*: At +140 mV the open-channel noise is much larger and more flickery than that measured at +60 mV. This indicates unresolved fast gating (Hille, 1992; Hansen

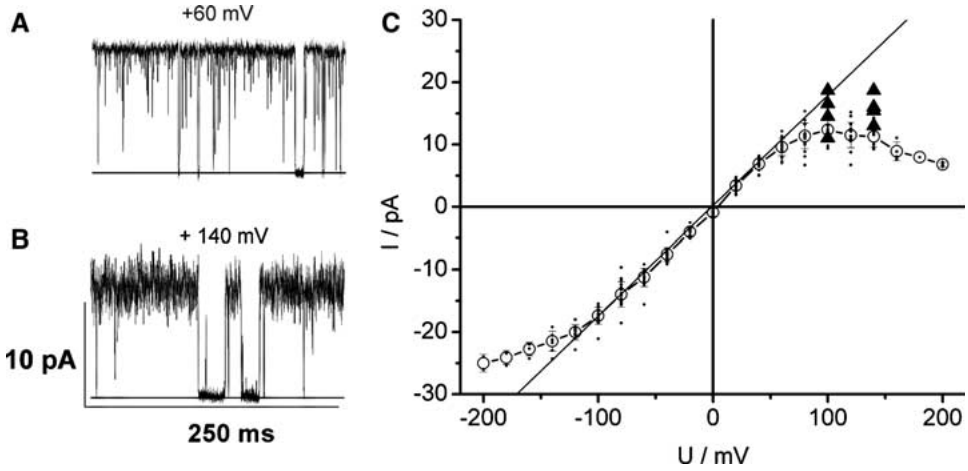

Fig. 7. Reconstruction of true single-channel currents in the range of the negative slope of the MaxiK IV-curve in symmetric 150 mM K^+. Time series obtained (A) in the linear range of the IV-curve and (B) in the negative slope. (C) Measured and reconstructed single-channel currents. (•) = data points from individual patches (note the large scatter). (○) = mean values (SEM) of measured current. (▲) = reconstructed currents of some individual current recordings.

et al., 1997; Townsend & Horn, 1999). +60 mV is still in the linear range of the *I-V* curve, whereas at +140 mV the negative slope is very prominent.

Again, true-current reconstruction was based on fitting the open-histogram by means of an *OC*-model. Applying this method to several time series within the negative slope led to the triangles in Fig. 7*C*. Some of them reached the extrapolated linear *I-V* curve. Some, however, showed increased current, but it did not reach the linear *I-V* curve. This may indicate that a second process like saturation may be involved as discussed below.

Discussion

Using Beta Distributions for Current Reconstruction

Fast gating and the related averaging over closed and open intervals in the inevitable low-pass filter of the experimental set-up can cause severe differences between measured apparent single-channel current and true single-channel current, as illustrated in Fig. 3. Fortunately, this reduction in current is coupled to a distortion of the curve shape of the related amplitude histograms. In Fig. 4, it is shown by means of simulated data that the error sum (Eq. 3) resulting from the comparison of the amplitude histograms of measured and reconstructed time series strongly depends on the assumption of the correct true single-channel current. This is a solid basis for the reconstruction of the hidden true single-channel current.

One finding presented in Fig. 4 and Table 2 is very important, namely that the distributions-per-level can be fitted with a smaller model than used for the analysis of the kinetics, i.e., for the determination of the rate constants of the assumed Markov model. Using a smaller model increases the stability of the fit. From the shape of Beta distributions, only a very small number of parameters can be determined. In the successful approaches above (Fig. 4 and Table 2) this is restricted to 3 or 5, i.e., one or two pairs of rate constants and one current value.

Reconstruction of the true single-channel current adds a new competency to the repertoire of Beta distributions. So far, they were employed for the determination of the rate constants of very fast gating processes (Fitz Hugh, 1983; Yellen, 1984; Heinemann & Sigworth, 1991; Klieber & Gradmann, 1993; Tsushima, Kelly & Wasserstrom, 1996; White & Ridout; 1998; Weise & Gradmann, 2000; Schroeder et al., 2004; 2005). They enable one to look far beyond the corner frequency of the anti-aliasing filter, i.e., dwell times in the range of 1 μs were obtained from time series filtered by 50 kHz.

Distributions-per-Level

Interestingly, better results were obtained by using distributions-per-level instead of the overall-amplitude histograms (Fig. 4). This is not a surprise as the exclusion of sections with long sojourns in a full state decreases the number of relevant states in the Markov model and thus allows fitting with a smaller one. The frequent failure of larger models is described by White and Ridout (1998) with the words "In a three-state model the precision of estimates depended in a complex way on all rate parameters in the model". Here, a welcome side effect of the normally undesired limited time resolution of the jump detector is utilized. When gating becomes fast,

the detector is no longer able to realize the short sojourns in the closed state occurring during a burst. Thus the fast events originating from a small part of the complex Markov model (mainly an OC-model) are merged into one apparent open level. The related section of the time series can be modelled with an *OC*-model with a very short-lived closed state (*see* Fig. 4).

It should be mentioned that fitting distributions-per-level with a reduced number of states may lead to severe errors in the determination of the rate constants (Table 2, last two rows). In distributions-per-level, not only the sojourns in the slow (closed) states are omitted, but also those of the faster states, which occur in the tail of the dwell-time distribution. Because of this, the kinetic analysis delivering the rate constants should be repeated utilizing the knowledge of the reconstructed true current obtained from the Beta fit. For this purpose, the HHM-fit as suggested by the Sigworth group (Venkataramanan & Sigworth, 2002), the *SQ*-fit (Schroeder et al., 2005) or the 2-D dwell-time fit (Magleby & Weiss, 1990; Huth, 2005) is recommended.

Even though the usage of distributions-per-level may lead to errors in the determination of the rate constants, all simulations done so far yielded a correct estimation of the true current level as shown in Figs. 4 and 5, and Table 2.

The Benefit of Current Reconstruction

The importance of estimating the correct true current level is illustrated by means of two examples. For a kinetic analysis, Fig. 1 and Table 1 illustrate that fitting a time series under different assumptions for the original single-channel current can lead to completely different rate constants. There have been several successful approaches to determine simultaneously both rate constants and current (Michalek, Wagner & Timmer, 2000; Qin, Auerbach & Sachs, 2000; Venkataramanan & Sigworth, 2002). Here, we have proposed an alternative approach, i.e., determining the current first, and fitting the rate constants in a second step. This method has two advantages: First, simple algorithms are much faster than more sophisticated programs. The current reconstruction takes 1 min to 1 h (depending on the length of the time series and the rate constants; the simulation is the time-consuming step) on a personal computer (1.4 GHz, 512 MB RAM). The simple HMM-fit (Fredkin & Rice, 1992; Albertsen & Hansen, 1994) using the reconstructed current takes approximately the same time. Consequently, this procedure is adequate for the analysis of a large number of time series. Second, most fitting programs, especially the Beta-fit, tend to get unstable with large parameter sets. Thus, splitting the fitting procedure in two parts improves the stability.

Limitations in Real Data

In the last three sections (Figs. 6 and 7), it has been shown that the success of this method of current reconstruction is not restricted to idealized simulated data. The application on measured data, too, yields reliable results. However, these data have to be of excellent quality. The baseline noise should be as low as possible. Otherwise, the excess noise (resulting from gating) can no longer be distinguished from the basic noise. Additionally, the time series must be absolutely drift-free, because even a tiny drift would distort the amplitude histogram. Alternatively, the use of a very good drift elimination algorithm may overcome this problem.

The limiting role of the signal-to-noise ratio becomes obvious in the data presented in the last section. The deviation from the linear *I-V* curve in Fig. 7*C* at positive potentials may originate from three putative mechanisms: (*A*) A permeation effect resulting in the negative slope. (*B*) A saturation effect which would explain only part of the current reduction or (*C*) a gating effect explaining all or part of the current reduction. The analysis could show that there is current reduction by fast gating in the negative slope of MaxiK. However, the question remains open of whether fast gating alone can explain the complete amount of the deviation from the extrapolated linear *I-V* curve. The problems arise from the strict requirements concerning the quality of the data, as mentioned above. When the noise is too high the determination of the true current does not reach a sufficient accuracy. Furthermore, due to seal instabilities, the quality of the data obtained at membrane potentials higher than +140 mV was not good enough for fitting. Thus it remains open whether in addition to the gating effect verified by the analysis also a saturation effect has to be assumed.

Such a saturation effect can be caused, e.g., by diffusion limitation at the entrance of the pore (Laver, Fairley & Walker, 1989; Laver & Fairley-Grenot, 1994) or a cyclic reaction scheme for ion transport, as suggested by Hansen et al. (1981) or Gradmann, Klieber & Hansen (1987). This would imply that the channel configuration has to relax after each passage of an ion. To fully solve this problem, the baseline noise needs further reduction in order to enable a clearer separation between the baseline noise and the excess noise caused by fast gating.

Appendix

Construction of the Theoretical Beta Distribution by Simulation of Surrogate Time Series

White and Ridout (1998) constructed the theoretical beta distributions as follows: From a suggested multi-

state hidden Markov model a short sequence of events was generated, which was as long as the filter response. For this sequence, the average current and the likelihood of the occurrence of this sequence were calculated. After superimposing gaussian noise, the beta distribution was obtained from the sum over the gaussian distributions of all possible sequences, weighted with their individual likelihood.

The availability of increased computer speed enables the usage of an alternative approach: Surrogate time series are used for the generation of theoretical amplitude histograms and as "measured data" when algorithms have to be tested. The basic approach of generating time series from a selected Markov model with an assumed set of states and rate constants has been described in previous papers (Blunck et al., 1998; Caliebe, Rösler & Hansen, 2002; Riessner et al., 2002; Schröder et al., 2004, 2005, program available at www.zbm.uni-kiel.de/software).

Briefly, a Markov model and the related rate constants of the transitions have to be assumed. For the calculation of the time series, two random numbers have to generated: The first one ($n_1 \epsilon [0,1]$) is used to calculate the time of the next jump (Δt) from the source state R_r to the sink (destination) state R_S in continuous time, with k_{rs}, k_{sr} being the rate constants of the transitions between R_s and R_r. Jump time Δt is obtained from the random number n_1 by an inversion of the dwell time distribution of the source state R_r

$$\Delta t = -\frac{1}{K_{rr}} \ln (n_1) \text{ with } \sum_{s \neq r} k_{rs} = -k_{rr} \qquad (A.1)$$

s labels all possible sink states for a jump out of the present state R_r. The second random number n_2 (uniformly distributed, $0 \leq n_2 \leq 1$) gives the target of the jump (sink state R_s). After the time interval Δt the jump occurs, and two new random numbers are generated to repeat the procedure.

This work was supported by the Deutsche Forschungsgemeinschaft Ha712/14-1,2. We are grateful to Imke Diddens for critical reading.

References

Albertsen, A., Hansen, U.P. 1994. Estimation of kinetic rate constants from multi-channel recordings by a direct fit of the time series. *Biophys. J.* **67:**1393–1403

Beilby, M.J. 1985. Potassium channels at *Chara* plasmalemma. *J. Exp. Bot.* **36:**228–239

Blunck, R., Kirst, U., Rießner, T., Hansen, U.P. 1998. How powerful is the dwell time analysis of multi-channel records? J. *Membrane Biol.* **165:**19–35

Caceci, M.S., Cacheris., W.P. 1984. Fitting curves to data — the simplex algorithm is the answer. *BYTE* **5/84:**340–362

Caliebe, A., Rösler, U., Hansen, U.P. 2002. A χ^2 test for model determination and sublevel detection in ion channel analysis. *J. Membrane Biol.* **185:**25–41

Crouzy, S.C., Sigworth, F.J. 1990. Yet another approach to the dwell-time omission problem of single-channel analysis. *Biophys. J.* **58:**731–743

Draber, S., Hansen, U.P. 1994. Fast single-channel measurements resolve the blocking effect of Cs^+ on the K^+ channel. *Biophys. J.* **67:**120–129

Draber, S., Schultze, R. 1994. Correction for missed events based on a realistic model of a detector. *Biophys. J.* **66:**191–202

Feller W. 1968. An Introduction to Probability Theory and Its Applications, Vol. 1, *John Wiley & Sons*

Farokhi, A., Keunecke, M., Hansen, U.P. 2000. The anomalous mole fraction effect in *Chara*: Gating at the edge of temporal resolution. *Biophys. J.* **79:**3072–3082

Fredkin, D.R., Rice, J.A. 1992. Maximum likelihood estimation and identification directly from single-channel recordings. *Proc. Roy. Soc. Lond. B* **249:**125–132

Fredkin, D.R., Rice, J.A. 2001. Fast evaluation of the likelihood of an HMM: Ion channel currents with filtering and colored noise: *IEEE Trans. Sig. Proc.* **49:**625–633

FitzHugh, R. 1983. Statistical properties of the asymmetric random telegraph signal with application to single-channel analysis. *Mathem. Biosci.* **64:**75–89

Gradmann, D., Klieber, H.-G., Hansen, U.-P. 1987. Reaction-kinetic parameters for ion transport from steady-state current-voltage curves. *Biophys. J.* **51:**569–585

Hansen., U.P., Cakan, O., Abshagen-Keunecke, M., Farokhi, A. 2003. Gating models of the anomalous mole fraction effect of single-channel current in *Chara*. *J. Membrane Biol.* **192:**45–63

Hansen, U.P., Keunecke, M., Blunck, R. 1997. Gating and permeation models of plant channels. *J. Exp. Bot.* **48:**365–382

Hansen, U.P., Gradmann, D., Sanders, D., Slayman, C.L. 1981. Interpretation of current-voltage relationships for "active" ion transport systems: I. Steady-state reaction-kinetic analysis of Class-I mechanisms. *J. Membrane Biol.* **63:**165–190

Heinemann, S.H., Sigworth, F.J. 1991. Open channel noise. VI. Analysis of amplitude histograms to determine rapid kinetic parameters. *Biophys. J.* **60:**577–587

Hille, B. 1992. Ionic Channels of Excitable Membranes. Sinauer Associates Inc., Sunderland, MA

Huth T. 2005. 4-Mode-Gating-Modell: Modellierung der Inaktivierung des Natriumkanals. PhD thesis, Kiel, www.zbm.uni-kiel.de

Klieber, H.G., Gradmann, D. 1993. Enzyme kinetics of the prime K^+ channel in the tonoplast of *Chara*: selectivity and inhibition. *J. Membrane Biol.* **132:**253–265

Korn, S.J., Horn, R. 1988. Statistical discrimination of fractal and Markov models of single-channel gating. *Biophys. J.* **54:**871–877

Laver, D.R, Fairley-Grenot, K.A. 1994. Surface potentials near the mouth of the large-conductance K^+ channel from *Chara australis*. A new method of testing for diffusion-limited ion flow. *J. Membrane Biol.* **139:**149–165

Laver, D.R., Fairley, K.A., Walker, N.A. 1989. Ion permeation in a K^+ channel in *Chara australis:* Direct evidence for diffusion limitation of ion flow in a maxi-K channel. *J. Membrane Biol.* **108:**153–164

Lehmann-Horn, F., Jurkat-Rott, K. 1999. Voltage-gated ion channels and hereditary disease. *Physiol. Rev.* **79:**1317–1372

Magleby, K.L., Weiss, D.S. 1990. Identifying kinetic gating mechanisms for ion channels by using two-dimensional distributions of simulated dwell times. *Proc. R. Soc. Lond. B* **241:**220–228

Moss, B.L., Magleby, K.L. 2001. Gating and conductance properties of BK channels are modulated by the S9-S10 tail domain of the α-subunit. A study of mSlo1 and mSlo3

wild-type and chimeric channels. *J. Gen. Physiol.* **118:**711–734

Michalek, S., Wagner, M., Timmer, J. 2000. A new approximate likelihood estimator for ARMA-filtered hidden Markov-models. *IEEE Trans. Sig. Proc.* **48:**1537–1547

Milne, R.K., Yeo, G.F., Madsen, B.W., Edeson, R.O. 1989. Estimation of single channel kinetic parameters from data subject to limited time resolution. *Biophys. J.* **55:**673–676

Parzefall, F., Wilhelm, R, Heckmann, M., Dudel, J. 1998. Single-channel currents at six microsecond resolution elicited by acethylcholine in mouse myoballs. *J. Physiol.* **512:**181–188

Press, W.H., Flannery, B.P., Teukolsky, S.A., Vetterling, W.T. 1987. Numerical Recipes. The Art of Scientific Computing. Cambridge University Press, Cambridge, New York, New Rochelle, Melbourne, Sidney

Qin, F., Auerbach, A., Sachs, F. 2000. Hidden Markov modelling for single-channel kinetics with filtering and correlated noise. *Biophys. J.* **79:**1928–1944

Riessner, T. 1998. Level Detection and Extended Beta Distributions for the Analysis of Fast Rate Constants of Markov Processes in Sampled Data. *PhD Thesis, Kiel, Germany and Shaker-Verlag, Aachen*

Riessner, T., Woelk, F., Abshagen, M., Hansen, U.P. 2002. A new level detector for ion channel analysis. *J. Membrane Biol.* **189:**105–118

Rosenmund, C., Stern-Bach, Y., Stevens, C.F. 1998. The tetrameric structure of a glutamate receptor channel. *Science* **280:**1596–1599

Schroeder, I., Harlfinger, P., Huth, T., Hansen, U.P. 2005. A subsequent fit of time series and amplitude histogram of patch clamp data reveals rate-constants up to 1 μs^{-1}. *J. Membrane Biol.* **203:**83–99

Schroeder, I., Huth, T., Suitchmezian, V., Jarosik, J., Schnell, S., Hansen, U.P. 2004. Distributions-per-level: A means of testing level detectors and models of patch clamp data. *J. Membrane Biol.* **197:**49–58

Schultze, R., Draber, S. 1993. A nonlinear filter algorithm for detection of jumps in patch-clamp data. *J. Membrane Biol.* **132:**41–52

Shi, J., Cui, J. 2001. Intracellular Mg^{2+} enhances the function of BK-type Ca^{2+}-activated K^+ channel. *J. Gen. Physiol.* **118:**589–605

Shieh, C.C., Coghlan, M., Sullivan, J.P., Gopalakrishnan, M. 2000. Potassium channels: Molecular defects, diseases, and therapeutic opportunities. *Phamacol. Rev.* **52:**557–593

Smith, J.R. 1984. Electrical evidence from perfused and intact cells for voltage-dependent K^+ channels in the plasmalemma of *Chara australis*. *Aust. J. Plant Physiol.* **11:**303–318

Tamargo, J., Caballero, R., Gomez, R., Valenzuela, C., Delpon, E. 2004. Pharmacology of cardiac potassium channels. *Cardiovasc. Res.* **62:**9–33

Tester, M. 1988. Blockade of potassium channels in the plasmalemma of *Chara corallina* by Tetraethylammonium, Ba^{2+}, Na^+ and Cs^+. *J. Membrane. Biol.* **105:**77–85

Townsend, C, Horn, R. 1999. Interaction between the pore and the fast gate of the cardiac sodium channel. *J. Gen. Physiol.* **113:**321–331

Tsushima, R.G., Kelly, J.E., Wasserstrom, J.A. 1996. Characteristics of cocaine block of purified sacroplasmic recticulum calcium release channels. *Biophys. J.* **70:**1263–1274

Venkataramanan, L., Sigworth, F.J. 2002. Applying hidden Markov models to the analysis of single ion channel activity. *Biophys. J.* **82:**1930–1942

Weise, R., Gradmann, D. 2000. Effects of Na^+ on the predominant K^+ channel in the tonoplast of *Chara*: Decrease of conductance by blocks in 100 nanoseconds range and introduction of oligo- or poly-subconductance gating modes. *J. Membrane Biol.* **175:**87–93

White, P.J., Ridout, M.S. 1998. The estimation of rapid rate constants from current-amplitude frequency distributions of single-channel recordings. *J. Membrane Biol.* **161:**115–129

Yellen, G. 1984. Ionic permeation and blockade in Ca^{2+} activated K^+ channels of bovine chromaffin cells. *J. Gen. Physiol.* **84:**157–186

Zheng, J., Venkataramanan, L., Sigworth, F.J. 2001. Hidden Markov model analysis of intermediate gating steps associated with the pore gate of Shaker potassium channels. *J. Gen. Physiol.* **118:**547–562